NASA TECHNICAL MEMORANDUM

NASA TM X- 71459

NASA TM X- 71459

EXPERIMENTAL AND THEORETICAL INVESTIGATION OF HT-S/PMR-PI COMPOSITES FOR APPLICATION TO ADVANCED AIRCRAFT ENGINES

by M. P. Hanson and C.C. Chamis
Lewis Research Center
Cleveland, Ohio 44135

TECHNICAL PAPER proposed for presentation at
Twenty-ninth Reinforced Plastics Technical and Management Conference sponsored by the Reinforced Plastics/Composites Institute of the Society of the Plastics Industries, Inc.
Washington, D.C., February 5 - 8, 1974

EXPERIMENTAL AND THEORETICAL INVESTIGATION OF HT-S/PMR-PI COMPOSITES FOR APPLICATION TO ADVANCED AIRCRAFT ENGINES

by M. P. Hanson* and C.C. Chamis*

Lewis Research Center

E-7700

ABSTRACT

A combined experimental and theoretical investigation was performed in order to: (1) demonstrate that high quality angleplied laminates can be made from HT-S/PMR-PI (PMR in situ polymerization of monomeric reactants), (2) characterize the PMR-PI material and to determine the HT-S unidirectional composite properties required for composite micro and macromechanics and laminate analyses, (3) select HT-S/PMR laminate configurations to meet the general design requirements for high-tip-speed compressor blades. The results of the investigation showed that: HT-S/PMR laminate configurations can be fabricated which satisfy the high-tip-speed compressor blade design requirements when operating within the temperature capability of the polyimide matrix.

---

*Aerospace Engineer, NASA Lewis Research Center, Cleveland, Ohio.

INTRODUCTION

Advanced aircraft engines designed with high-speed axial-flow compressor stages, will require high performance composites with high strength retention at elevated temperatures. Preliminary investigation of HT-S/PMR-PI composites (ref. 1) showed that these composites have the potential for meeting the requirements for advanced engine compressors which operate within the temperature capability of the PMR-PI resin.

In order to establish the suitability of HT-S/PMR-PI composites for advanced aircraft engine applications a combines experimental and theoretical investigation was performed. The objectives of the investigation were: (1) to demonstrate that high quality angleplied laminates can be made from HT-S/PMR-PI (PMR in situ polymerization of monomeric reactants) composites, (2) to characterize the PMR-PI material and to determine the HT-S unidirectional composite properties required for composite micro and macromechanics and laminate analyses, (3) to select HT-S/PMR-PI laminate configurations to meet the design requirements for high-tip-speed compressor blades.

The combined experimental and theoretical investigation was performed in the following manner. Test specimens were made from the PMR neat resign and from HT-S/PMR-PI unidirectional composites. HT-S/PMR-PI laminates were made with ply configurations simulating those considered for high-tip-speed compressor blade applications. The coefficients of thermal expansion and mechanical properties; i.e., izod impact, tensile and flexural strengths, and stiffness of the PMR-PI resin and HT-S fiber composites were evaluated and used in the laminate analysis and composite macro and micromechanics. The simulated

blade laminates were tested to fracture in tension and flexure. Laminate analysis and composite macro and micromechanics were used to calculate the stresses in the plies due to: lamination residual stresses, applied load to fracture, and the combination of the two. Available combined-stress strength criteria were used to determine the margin of safety or failure of the plies under applied load. The properties of blade-type laminates were compared with the general design requirements for ultra high-tip-speed composite compressor blades.

EXPERIMENTAL PROGRAM

The experimental program was undertaken to determine mechanical properites as related to the application of graphite-fiber/polyimide resins to advanced aircraft engine applications. The results are used to verify quantitatively the theoretical considerations and concepts described in the Theoretical Investigation. Materials evaluated were of the neat resin and graphite/resin composites in various ply orientations.

MATERIALS AND SPECIMEN FABRICATION

Neat Resin

The monomer solution was formulated from the monomeric reactants (1) 4,4'-methylenedianiline (MDA), (2) monomethylester of 5-norbornene-2, 3-dicarboxylic acid (NE) and dimethylester of 3, 3', 4, 4' benzophenonetetracarboxylic acid (BTDE) with methyl alcohol as the solvent. The solution was prepared according to the procedure reported in ref. 1 (sample 1).

Molded neat resin was prepared by drying the solution and grinding to a powder. The powder was then imidized at 204^{o}C (400^{o}F) for 2 hours. The powder was placed in a cold mold and compacted under 345 N/cm^{2} (500 psi) pressure. With the pressure released, the mold

was heated to 274C (525°F). At this point a mold pressure of 345N/cm^2 (500 psi) was applied and the temperature increased to 316C (600°F). After 1 hour the resin was cured.

Laminate Fabrication

The HT-S fiber was drum wound and impregnated with the PMR-PI resin. The resin was in a solvent solution having a solids content of 50 percent by weight. A predetermined quantity of resin solution was applied to the fiber so that the final cured laminate would have a fiber volume content of 55 percent. Heat lamps were used to reduce the solvent content to approximately 10 percent before removing the prepreg from the drum. The prepared prepreg had a thickness of 0.20 mm (0.008 inch). Unidirectional and various angleplied were cut to mold size 7.62 x 25.4 cm (3 x 10 inch) to fabricate the laminates listed in Table 2.

The plies were stacked between porpous TFE-coated glass-cloth, placed in a mold sized tray and compacted with a 4.53 K_g (10 pound) weight. The preform was imidized in an air-circulating oven at 204 C (400°F) for 2 hours. The TFE-coated glass-cloth was removed and the preform was placed between aluminum caulplates and placed in the preheated 204C (400°F) mold. The cure cylce is shown graphically in figure 1. Since the laminate exhibits a thermoplastic behavior in the "as cured" condition, all laminates were post cured as noted in figure 1.

Specimen Fabrication

Neat-resin tensile specimens were machined from 3.2 mm (0.125-inch) thick material in accordance with ASTM standard method D638-type 1. Compression specimens were machined from coupons 12.7 x 38 mm (0.5 x 1.5 inch) to provide a test section 6.3 mm (0.25 inch) wide by 19.1 mm (0.75 inch) long.

Longtitudinal tensile specimens of the HT-S/PMR-PI were machined having dimensions of 1.27 x 25.4 cm (0.5 x 10 in.) from the 7.62 x 25.4 cm (3 x 10 inch) laminates with the 0^{o} fiber plies in the 25.4 cm (10 inch) direction. The specimens had parallel sides with 6.3 cm (2.5 inch) long reinforcing tabs adhesively bonded to the ends. Transverse tensile specimens were machined from 12.7 mm (0.5 inch) wide by 7.6 cm (3 inch) long coupons. The finished specimen had a reduced test section 6.3 mm (0.25 inch) wide by 38 mm (1.5 inch) long. 6.3 mm (0.25 inch) reinforced holes on the ends were provided for load application.

Miniature Izod specimens were machined from 0^{o} ply composites 5.1 mm (0.20 inch) thick. The finished specimen dimensions were 5.1 x 5.1 x 37.6 mm (0.2 x 0.2 x 1.48 inch).

TEST APPARATUS AND PROCEDURE

Tensile, flexure and interlaminar shear tests were performed in a universal testing machine with a selected constant-speed crosshead.

Tensile tests of the neat resin were performed in accordance with ASTM method D638 at a crosshead speed of 2.5 mm (0.1 inch) per minute. The various composite tensile specimens were tested at 1.3 mm (0.05 inch) per minute. Strain to fracture was measured with a clamp-on extensometer.

The flexure specimens were tested using the ASTM standard method D709-71- Method I. Teste were made on a three point loading fixture having a span of 5.1 cm (2.0 inch). The short-beam interlaminar shear specimens were tested using a three-point loading fixture having a span to thickness ratio of 5:1.

Izod impact specimens were tested in a modified Bell Telephone Laboratory pendulum type machine. The striking velocity of the pendulum

was 345 centimeters (136 inches) per second. The Izod specimens were struck at their free end, 22 mm (0.87 inch) from the edge of the cantilever grip.

The coefficients of thermal expansion were determined for the neat resin and longitudinal and transverse uniaxial composite material. Coupons of resin and composite were heated from 38C (75^{o}F) to 316C (600^{o}F) and the change in dimension was measured using imbedded thermocouples.

EXPERIMENTAL RESULTS AND DISCUSSION

The results obtained from the experimental investigation of neat resin and composite material consist of stress/strain diagrams, and mechanical and physical properties.

The stress/strain diagram of the PMR-PI neat resin is shown in figure 2. As can be seen the relation is essentially linear to fracture. The modulus of the neat resin 0.33×10^{6} N/cm^{2} (0.47×10^{6} psi) is a typical value of PI resin systems. The stress/strain diagrams of the various angleplied composites are shown in figure 3. It can be seen that the modulus of 15.0×10^{6} N/cm^{2} (21.7×10^{6} psi) is typical of uniaxial HT-S composites with 55 percent fiber volume. It is also noted that the two composites with 10^{o} plies have moduli similar to the uniaxial composite (14.6×10^{6} and 13.1×10^{6} N/cm^{2}) (21.1×10^{6} and 19.0×10^{6} psi). The $\pm 40^{o}$ and 0^{o} ply laminate shows a lower modulus than would be expected with the predominance of 0^{o} plies. Possible causes for this behavior will be discussed in the Theoretical Program section.

Tables 1 and 2 summarize the strength properties of the neat resin and composite materials. The data are an average of three or more tests

of the particular property. Although most of the strength properties are comparable to that reported of neat resins and HT-S composite materials the tensile strength reported of the neat resin may be lower than the actual value due to inherent limitation of the molding qualities of the resin. Also the low compressive strength of the composite material may not be a realistic value because the inherent limitations of the test method.

THEORETICAL PROGRAM

The theoretical program consisted of two parts: (1) selection of the correlation coefficients required in the Computer Code (ref. 2) to carry out the composite micro and macromechanics and (2) laminate analysis of the various laminates tested. These parts are essential in assessing both the potential of the HT-S/PMR-PI composite for high-tip-speed compressor blade applications and the in situ PMR-PI matrix performance. The notation used herein is defined when it first appears and it is summerized under symbols at the end of the text for convenience.

SELECTION OF CORRELATION COEFFICIENTS

Two sets of correlation coefficients are needed in the Computer Code (ref. 2). The first set is required for the prediction of unidirectional composite thermal and elastic properties from corresponding constituent properties. The second set is required for the prediction of unidirectional composite strength properites.

Correlation Coefficients for Thermal and Elastic Properties

The constituent material properties required to predict composite properties from constituent properties using composite micromechanics

are summarized in Table 3. The correlation coefficients for thermal and elastic properties were the same as those for type II-fiber/resin matrix composites. See reference 2, Table XI. This is consistent with previous experience (ref. 3) where it was found that the correlation coefficients for elastic and thermal properites appear to be insensitive to fiber-resin types.

Correlation Coefficients for Unidirection Composite Strengths

Five unidirectional composite strengths are required to characterize a unidirectional composite from the strength viewpoint. These strengths are: longitudinal tension ($S_{\ell 11T}$), longitudinal compression ($S_{\ell 11C}$), transverse tension ($S_{\ell 22T}$), transverse compression ($S_{\ell 22C}$) and intralaminar shear ($S_{\ell 12S}$). These strengths can be predicted from corresponding constituent properties using composite micromechanics. The main advantage for relating composite strength to constituent properties is that the micromechanics in the computer code provides for in sity ply strength. The constituent material properties required for predicting the aforementioned strengths via micromechanics are summarized in Table 4. The values of the correlation coefficients used in the computer code are listed in Table 5.

Two important points can be made from the values of the strength correlation coefficients in Table 5. These are:

1. The value of $\beta_{fT} = 0.94$ which is close to unity. This indicates a relatively high matrix efficiency in translating fiber strength to composite.

2. The values of the strength correlation coefficients β_{22T}, β_{22C} and β_{12S} are unity or higher. These indicate that the in situ PMR-PI

matrix strength is equal to or better than its bulk state strength. This latter point attains additional importance since the values of these strength correlation coefficients are about 0.5 for other fiber/resin composites.

The important conclusion from the preceding discussion is: in situ polymerization appears to enhance the fiber/matrix interfacial bond and the in situ matrix strength resulting in improved intralaminar shear and transverse tensile strengths for the unidirectional composite.

Measured and predicted unidirectional composite properties are summarized in Table 6 for comparison purposes. Some items in Table 6 need additional explanation.

1. No measured data are available for the thermal heat conductivities for the composite or the PMR-PI matrix. The predicted values shown in Table 6 are based on the estimated matrix data shown in Table 3. They are included here as indications. Also, no measured data are available for composite shear modulus or Poisson's ratio.

2. The limiting value of the transverse compressive stress (S_{l22C}) was taken to be about 80% of the corresponding fracture stress. This was done because in general transverse compression stress/strain curves exhibit excessive nonlinearities beyond the 80% fracture stress value.

3. The intralaminar shear strength (S_{l12S}) was taken to be about 50% of the short-beam-shear fracture stress value. This was done for two reasons: (a) In house results of angleplied laminate analyses has indicated that in predominatly shear-failed laminates the intralaminar shear stress was about one-half of the short-beam-shear fracture stress.

(b) S-glass fiber/resin unidirectional thin tubes subjected to torsion fracture at a shear stress which is about 50 to 60% of the corresponding short-beam-shear fracture stress.

By examining the measured and predicted property values in Table 6 it can be seen that the correlation coefficients selected yield predicted values which are in good agreement with the measured data.

The afore discussion leads to the following tentative recommendation. The intralaminar shear strength to be taken at one-half the short-beam-shear (interlaminar) fracture stress.

LAMINATE ANALYSIS OF ANGLEPIED LAMINATES

The laminate analysis capability available in the Computer Code (ref. 2) was used to analyze the laminates tested. The laminate analysis performed yielded the following laminate properties: (1) thermal and elastic constants, (2) plate-type bending stiffnesses, and (3) the ply stresses and margin-of-safety due to cure temperature, axial fracture load, bending fracture moment, and combinations. This type of information serves two purposes:

1. To assess the application of linear laminate theory to HT-S/PMR-PI composites.
2. To establish whether any or all of the laminates investigated meet the general design requirements of the high-tip-speed compressor blade.

Laminate Elastic Constants and Thermal Coefficients of Expansion

The elastic constant and thermal coefficients of ecpansion of the laminate were calculated using the unidirectional composite properties in Table 6. The results are summarized in Table 7. The information in Table 7 can be used to select ply arrangement for the blade core and

the blade shell. Based on composite blade general design requirements to be described later the laminates 6[0], 4[$\pm$ 10, $\mp$ 10], and 8[0, +10, 0, -10, -10, 0, +10, 0] are suitable for the blade core while the laminate 4[$\pm$ 40 $\mp$ 40] is suitable for the blade shell. The laminate 13[$\pm$ 40, 9 (0), $\mp$ 40] is representative of the blade at its maximum thickness point. This laminate has a negative thermal coefficient of expansion along the x-direction (α_{cxx}). This is an added advantage because it counteracts the radial growth of the blade due to centrfugal loads.

Three other points need to be mentioned with regard to Table 7.

1. The laminate properties in Table 7 are based on 0.55 fiber volume ratio. This value was selected because laminates from HT-S/PMR-PI under well controlled fabrication conditions are expected to have a fiber volume ratio of about 0.55.

2. Some laminates tested in this investigation could have had fiber volume ratios different than 0.55.

3. The predicted laminate moduli (E_{cxxx}) (Table 7) differ from the measured values in Table 2. This difference could be caused by any or combinations of the following factors: difference in fiber volume ratio, deviations in the ply orientation angle, deviations between actual and predicted shear modulus, bending due to testing load eccentricity and ply relative rotation.

The important point to be noted from the afore discussion is that HT-S/PMR-PI laminate configurations can be selected which appear to be suitable for compressor blade application from the thermo and elastic constants considerations. It should also be noted that the 8[0, +10, 0, -10, -10, 0, +10, 0] laminate has greater tensile strength

then the 6(0) laminate (Table 2). This indicates that the notch sensitivity of unidirectional composite with high interlaminar shear strength can be alleviated by orienting some of the plies at relatively low angles (10^{o} of less) to the load direction.

Laminate Plate Type Bending Stiffnesses

The plate-type bending stiffnesses are a good measure on how a fiber-composite compressor blade will perform when subjected to combined loadings and how they will resist vibrations and flutter. The plate-type bending stiffness of interest herein are the coefficients in the matrix equation:

$$\begin{Bmatrix} M_{cxx} \\ M_{cyy} \\ M_{cxy} \end{Bmatrix} = \begin{bmatrix} D_{c11} & D_{c12} & D_{c13} \\ D_{c21} & D_{c22} & D_{c23} \\ D_{c31} & D_{c32} & D_{c33} \end{bmatrix} \begin{Bmatrix} \kappa_{cxx} \\ \kappa_{cyy} \\ \kappa_{cxy} \end{Bmatrix} \qquad (1)$$

The notation in the last equation is as follows: M denotes moment; D, bending stiffness and κ, curvature. The subscript c denotes composite property. The subscripts xx, etc., represent structural axes directions. The subscripts 11 etc., represent positions in the array. The D array is symmetric that is $D_{c12} = D_{c21}$, $D_{c31} = D_{c13}$, and $D_{c32} = D_{c23}$. The physical meaning of the various D's is as follows: D_{c11} is the bending stiffness along the x-direction; D_{c22} is the bending stiffness along the y-direction; D_{c33} is the torsional stiffness; D_{c12} represents the bending resistance along the x-direction due to a moment in the y-direction; D_{c13} represents the bending resistance along the x-direction due to a torsional moment; D_{c23} represents the bending resistance along the y-direction due to a torsional moment. The symmetric coefficients

$D_{c_{21}}$, $D_{c_{31}}$, and $D_{c_{32}}$ have analogous physical meaning.

In fiber composite compressor blade design the bending stiffnesses are used to assess the following responses.

$D_{c_{11}}$ controls the tip deflection and the uncoupled span-wise vibration bending modes.

$D_{c_{22}}$ controls the uncambering and the uncoupled cord-wise vebration bending modes.

$D_{c_{33}}$ controls the untwist and the uncoupled twisting vibration modes.

The coefficients $D_{c_{12}}$, $D_{c_{13}}$, and $D_{c_{23}}$ control coupled responses indicated by the numerical subscripts.

In selecting laminate configurations for compressor blades, the procedure usually is as follows:

1. Select a laminate with a high value for $D_{c_{11}}$.
2. Adjust the ply orientations until the values for $D_{c_{22}}$ and $D_{c_{33}}$ are within a priori estimated ratios of $D_{c_{11}}$. The a priori estimated ratios depend on the span-to-cord ratio of the blade and could vary between 10 and 100 percent at the maximum blade thickness.
3. Retain ply orientations which yield relatively low values for the coupled coefficients $D_{c_{13}}$ and $D_{c_{23}}$.

It was mentioned in the last section that the laminate $13[\pm 40, 9(0), \mp 40]$ was a good candidate for the high-tip-speed compressor blade. The bending stiffnesses of this laminate are summarized in Table 8. Note that the values of $D_{c_{13}}$ and $D_{c_{23}}$ are relatively small compared to $D_{c_{11}}$. Note also that the values of $D_{c_{22}}$ and $D_{c_{33}}$ are about 25 to 30% of $D_{c_{11}}$. These values are consistant with the guidelines discussed

previously for selecting laminate configurations for compressor blade applications.

The laminate bending modulus can be obtained from the bending stiffness via the following equation:

$$E_{cxx} = 12D_{cxx}(1 - \nu_{cxy}\,\nu_{cyx})/t_c^3 \tag{2}$$

where

$$D_{cxx} = D_{c_{11}}$$

$$\nu_{cxy} = D_{c_{12}}/D_{c_{22}} \tag{3}$$

$$\nu_{cyx} = D_{c_{12}}/D_{c_{11}}$$

t_c = the laminate thickness.

Using values for $D_{c_{11}}$, $D_{c_{12}}$ and $D_{c_{22}}$ from Table 8 and t_c = .27 cm (0.106 in) in the equation for E_{cxx} yields 6.69×10^6 N/cm^2 (9.7×10^6 psi). The corresponding measured value from Table 2 is 6.41×10^6 N/cm^2 (9.3×10^6 psi) which is in good agreement with the predicted value.

Bending moduli were also computed for the other laminates tested. The predicted values for these laminates were about the same as the values for the E_{cxx} in Table 7. These values differ from the measured data. This difference could be caused by the factors causing the difference in the tensile moduli as mentioned in the last section. Additional factors which could cause difference between measured and predicted bending moduli are: relatively small numbers of plies (less than 10) which could violate the linear laminate theory assumptions, strong coupling between bending and twisting, and local indentation of the specimen at the support and bending points.

Two important conclusions follow from the previous dicsussion:

1. Laminate configurations for preliminary blade designs can be readily selected via laminate analysis when a priori estimates on the bending stiffnesses are available.
2. For angleplied laminates with relatively large numbers of plies (greater than 10), measured and predicted values of the bending modulus are in good agreement.

Conclusion number 2 is significant because it proves that linear laminate theory is applicalbe to angleplied laminates from HT-S/PMR-PI composites. It also provides confidence in the predicting blade deflections and frequencies via linear laminate theory.

Ply Stresses

The stresses and the margin-of-safety in the plies of the laminates investigated were determined using linear laminate theory. The linear laminate theory used is embedded in the Computer Code (ref. 2). The application of linear laminate theory for these calculations is valid because the laminates investigated exhibit linear stress-strain curves to fracture, figure 3.

Ply stresses and margins-of-safety were determined due to:

1. Cure temperature (residual stresses)
2. Axial fracture load with no residual stresses
3. Bending fracture moment with no residual stresses
4. Axial fracture load with residual stresses
5. Bending fracture moment with residual stresses.

The inputs for these calculations consisted of:

1. Constituent limit properties, Table 4
2. Strength correlation coefficcients, Table 5

3. Ply elastic and thermal properties, Table 6
4. Cure temperature difference which equals cure temperature minus room temperature, 295C ($530^{o}F$)
5. Specimen axial fracture load
6. Specimen bending fracture moment
7. Laminate configuration

The margin-of-safety was determined using a modified distortion energy principle for a combines-stress failure criterion (ref. 3).

The prupose of these calculations was to:

1. Assess the applicability of linear laminate theory to failure analysis of HT-S/PMR-PI anglepied laminates
2. Obtain an indirect assessment of the in situ ply strength
3. Determine whether the residual stresses would cause transply cracks.

The underlying consideration on the ply stress analysis calculations was the following: Fracture axial loads or bending moments, either singly or in combination with residual stresses, should produce ply combined-stress states with negative values for the margin-of-safety. This is a procedure which is employed to design structural components from angleplied laminates to satisfy strength requirements.

The ply stress calculation results are summarized in Table 9 for the $6[0]$ laminate; Table 10, for the $4[\pm 10, \mp 10]$ laminate; Table 11, for the $8[0, +10, 0, -10, -10, 0, +10, 0]$ laminate; and in Table 12, for the $13[\pm 40, 9(0) \mp 40]$ laminate. In these tables the type of loading and the ply at which stresses are listed in the columns headed by "Thermal Load Due to Cure". The stresses due to mechanical loads and no residual stress are listed in the columns headed by "Mechanical Load".

The combined stresses due to mechanical and thermal loads are listed in the columns headed by "Combined Loads".

The notation in these tables is as follows: $\sigma_{\ell 11}$ denotes ply stress along the fiber direction, $\sigma_{\ell 22}$ denotes ply stress transverse to the fiber direction, $\sigma_{\ell 12}$ denotes the in-plane (intralaminar) shear stress, and MOS denotes margin-of-safety as computed by the modified distortion energy principle mentioned previously. The first line of entry is in SI units and the second in customary units. The ply stresses due to axial force are entered in the top part of Tables 9-11, and those due to bending moment in the lower part. The ply stresses due to axial load are entered in Table 12a and those due to moment in Table 12b for the laminate $13[\pm 40,\ 9(0) \mp 40]$.

The three important points to be noted from the results shown in Tables 9-12 are:

1. The margin-of-safety for the residual stresses is positive for all the laminates. This indicates that the residual stresses do not cause transply cracks in the laminate configurations investigated.
2. The margin-of-safety is negative, or nearly so for one or more plies in each of the laminates when subjected to mechanical load only. This indicates that at fracture load or bending moment one or more of the plies failed.
3. The margin-of-safety is negative for one or more plies in each of the laminates for the combined load case. The values of the margins-of-safety for this case are more negative than for the mechanical-load-only case. This indicated a possible enchancement in the in situ ply strengths as was previously mentioned. It also indicates

that the presence of lamination residual stresses tent to decrease the load carrying capacity of the laminates.

The previous discussion leads to the following important conclusions with regard to HT-S/PMR-PI laminates representative for compressor blade applications:

1. Laminate failure as predicted by linear laminate theory is conservative.
2. There appears to be significant transverse and intralaminar shear strength enhancement in the in situ plies.
3. The lamination residual stresses do not cause transply cracks.

The above conclusions become even more significant because linear theory was used and the laminates investigated exhibited linear stress-strain curves to fracture.

An additional important conclusion follows from the ply stresses of the laminate $13[\pm 40, 9(0), \mp 40]$ in Tables 12a and 12b. As can be seen in these tables the zero plies have positive margine-of-safety. The conclusion, therefore, is that the zero plies are not utilized to their maximum efficiency. One way to alleviate this, is to intersperse a few 0^{o} plies with the shell plies.

APPLICATION OF HT-S/PMR-PI COMPOSITED TO ADVANCED AIRCRAFT ENGINES

A two phase procedure is used herein to determine the suitability of HT-S/PMR-PI composites for advanced aircraft engine application. In the first phase, we examine the general design requirements of the high-tip-speed compressor blade. In the second phase, we compare

the laminate properties obtained previously with the blade general design requirements. The criterion for establishing suitability is that one or more of the laminates investigated meet the blade general design requirements.

General Design Requirements for an Ultra High-Tip-Speed Compressor Composite Blade

The general design requirements for a high-tip-speed [671 m/sec (2200 ft/sec)] compressor blade from fiber composite materials are:

1. The core laminate configuration should have a tensile modulus of 12.4×10^6 N/cm^2 (18×10^6 psi) or greater.
2. The shell laminate configuration should have a shear modulus of 2.76×10^6 N/cm^2 (4×10^6 psi) or greater.
3. The core laminate configuration should have a tensile strength of 62.1×10^3 N/cm^2 (90 KSI) or greater at room temperature.
4. The blade laminate configuration shouls be free of transply cracks due to cure temperature.
5. The blade laminate configuration should retain its structural integrity in the temperature range -51C to 260C (-60^{o}F to 500^{o}F).
6. The unidirectional laminate should retain 70% or greater of its longitudinal tensile properties at about 288C (550^{o}F) for long time exposures; and it should retain 50% or greater of its other unidirectional properties.
7. The cordwise and torsional stiffnesses of the blade laminate configuration should be about 25 to 30% of the spanwise bending stiffness.
8. The blade laminate configuration should have good resistance to cyclic load.

9. The unidirectional laminate should have longitudinal Izod impact energy resistance of 113.0 cm-N (10 in-lb) or greater.

Comparison of Design Requirements with the Properties of the HT-S/PMR-PI Angleplied Laminates

Design requirements 1, 2 and 3 - Comparison of the measured or predicted stiffness/strength properties of the laminates 3[0], 4[$\pm$ 10, $\mp$ 10], 8[0, + 10, 0 - 10, - 10, 0, + 10, 0] indicate that these laminates meet these design requirements for the core. The predicted shear modulus for the laminate 4[$\pm$ 40 $\mp$ 40] meets the design requirements for the shell.

Design requirements 4 and 7 - The blade laminate configuration 13[$\pm$ 40, 9(0), $\mp$ 40] meets the residual stress requirements and the plate-type bending stiffness. It is noted that the average tensile strength of this laminate meets the design requirements of the core. And also, the modulus and tensile strength of this laminate are comparable to titanium alloys which are commonly used for compressor blades. This is significant since the titanium is three times heavier.

Design requirements 5 and 6 - The elevated temperature strength/stiffness retention of HT-S/PMR-PI unidirectional composites was investigated in reference 1. It was found that these composites retain about 70% of their room temperature flex stiffness/strength at 316C (600^{o}F) for long exposure times. The corresponging interlaminar shear strength retention was 50% or greater.

Design requirement 8 - Graphite fiber/non-metallic matrix composites have good cyclic load resistance. Unidirectional composites cyclic loaded at 80% of their static strength exceed 10^{6} cycles in general (ref. 4).

Design requirement 9 - The measured longitudinal Izod impact resistance for an HT-S/PMR-PI unidirectional laminate is 171.8 cm-N (15.2 in-lb), Table 2, which is 1.5 times greater than the design requirement.

The afore comparative discussion leads to the following conslusion. HT-S/PMR-PI laminates can be selected which meet all the general design requirements for a high-tip-speed composite compressor blade. Of the laminates investigated, the laminate $8[0, +10, 0, -10, -10, 0, +10, 0]$ is the best configuration for the blade core. The laminate configuration of $\pm 40^{o}$ interspersed with a few 0^{o} plies appears to be a good candidate for the shell.

CONCLUDING REMARKS

HT-S/PMR-PI laminates can be fabricated which meet all the general design requirements for a high-tip-speed composite compressor blade operatine within the temperature capability of the PMR-PI resin.

Of the laminates investigated for the 671 m/sec (2200 ft/sec) blade application, the laminate $8[0, +10, 0, -10, -10, 0, +10, 0]$ is the best configuration for the blade core and $\pm 40^{o}$ interspersed with a few 0^{o} -plies for the shell.

A combined experimental/theoretical investigation is the most direct approach to obtain a broad assessment of the application of new advanced composites to specific designs.

Laminate failure as predicted by linear laminate theory is conservative. There appears to be a significant transverse and intralaminar shear strength enhancement in the in situ plies. The lamination residual stresses do not cause transverse ply cracks in representative laminate configurations for compressor blade applications.

The in situ polymerization process enhances the fiber/matrix interfacial bond and the in situ matrix strength resulting in improved unidirectional composite transverse tensile and intralaminar shear strengths.

APPENDIX - SYMBOLS

a_1, a_2	unidirectional composite strength correlation coefficients, Table 5.
D	bending (flexural) stiffness, subscripts define type, Eq. 1
E	normal modulus, subscripts define type, Table 6
G	shear modulus, subscripts, define type, Table 6
K	thermal heat conductivities, subscripts define type, Tables 3 and 6
$K_{l\,12}$	coefficient for combined stress
M	bending moment, subscripts define direction, Eq. 1
S	unidirectional composite strength, subscripts define type and sense, Table 6
t_c	laminate (composite) thickness
α	thermal coefficients of expansion subscripts define type and direction, Tables 3, 6 and 7
β	correlation coefficients defined in Table 5
ϵ	strains, subscripts define type and direction
κ	curvatures, subscripts define type and direction
ν	Poisson's ratio, subscripts define type and direction Table 3, 6 and 7
ρ	density, subscripts define type, Table 3
σ	stress, subscripts define type and direction

SUBSCRIPTS

C	compression property
c	composite property
f	fiber property

l	unidirectional composite (ply) property
m	matrix property
p	limit value
S	shear property
T	tensile property
x, y, z	structural axes coordinate directions
1, 2, 3	type or material axes coordinate directions

REFERENCES

1. Delvigs, P., Serafini, T. T. and Lightsey, G. R.: Addition-Type Polyinides from Solutions of Monomeric Reactants, NASA TN D-6877, National Aeronautics and Space Administration, August, 1972.

2. Chamis C. C.: Computer Code for the Analysis of Multilayered Fiber Composites - Users Manual, NASA TN D-7013, National Aeronautics and Space Administration, March, 1971.

3. Chamis C.C.: Failure Criteria for Filamentary Composites, NASA TN D-5367, National Aeronautics and Space Administration, August, 1969.

4. Hanson, M. P.: Tensile and Load Cyclic Fatigue Properties of Graphite Filament Wound Pressure Vessels at Ambient and Chyogenic Temperatures. NASA TN D-5354, National Aeronautics and Space Administration, July, 1969.

TABLE 1. - ROOM TEMPERATURE PROPERTIES OF [a]PMR-PI NEAT RESIN

Tensile strength, N/cm^2 (psi)	5580 (8100)
Tensile modulus, N/cm^2 (psi)	0.32×10^6 (0.47×10^6)
Compressive yield strength, N/cm^2 (psi)	11 400 (16 500)
Compressive strength, N/cm^2 (psi)	18 700 (27 200)
Thermal coefficient of expansion, cm/cm/°C (in./in./°F)	50.4×10^{-6} (28.0×10^{-6})

[a] NE/MDA/BTDE (ref. 1) (1500 formulated molecular weight).

TABLE 2. - PROPERTIES OF HT-S/PMR-PI COMPOSITES

[55 Percent fiber volume and tested along the 0°-ply direction.]

Property	Ply angles, deg				
	6[0]	6[90]	4[± 10, ∓ 10]	8[0, + 10, 0, - 10 - 10, 0, + 10, 0]	13[± 40, 9(0), ∓ 40]
Tensile strength, N/cm^2 (psi)	124 000 (180 000)	6710 (9740)	103 400 (150 000)	131 500 (191 000)	85,400 (124 000)
Tensile modulus, N/cm^2 (psi)	15.0×10^6 (21.7×10^6)	0.79×10^6 (1.15×10^6)	14.5×10^6 (21.1×10^6)	13.1×10^6 (19.0×10^6)	9.6×10^6 (14.0×10^6)
Compressive strength, N/cm^2 (psi)	93 000 (135 000)	23 430 (34 000)	------	------	------
Flexural strength, N/cm^2 (psi)	141 900 (206 000)	11 270 (16 350)	158 500 (230 000)	135 700 (197 000)	99 900 (145 000)
Flexural modulus, N/cm^2 (psi)	12.1×10^6 (17.6×10^6)	0.74×10^6 (1.07×10^6)	11.6×10^6 (16.8×10^6)	13.1×10^6 (19.0×10^6)	6.4×10^6 (9.3×10^6)
Short-beam interlaminar shear, N/cm^2 (psi)	11 020 (16 000)	------	------	------	------
Miniature izod impact energy, cm-N (in.-lb)	171.8 (15.2)	20.3 1.8)	------	------	------
Coefficient of thermal expansion, cm/cm/C (in./in./°F)	~0	26.1 (14.5×10^{-6})	------	------	------

TABLE 3. - ELASTIC AND THERMAL PROPERTIES OF HT-S FIBER AND PMR-PI MATRIX CONSTITUENTS USED IN COMPOSITE MICROMECHANICS

Property	Symbol	Units		HT-S fiber		PMR-PI matrix	
		SI	Customary	SI	Customary	SI	Customary
Moduli	$E_{f(m)11}$	10^6N/cm^2	10^6 psi	26.2	38.0	.32	.47
	$E_{f(m)22}$	10^6N/cm^2	10^6 psi	1.4	2.0	.32	.47
	$G_{f(m)12}$	10^6N/cm^2	10^6 psi	1.7	2.5	.12	.17
Poisson's ratio	$\nu_{f(m)12}$	Ratio	Ratio	.25	.25	.36	.36
Thermal coefficients of expansion	$\alpha_{f(m)11}$	10^{-6}cm/cm/C	10^{-6}in./in./^{o}F	-.018	-.01	50.4	28.0
	$\alpha_{f(m)22}$	10^{-6}cm/cm/C	10^{-6}in./in./^{o}F	10.1	5.6	50.4	28.0
Heat conductivities	$\kappa_{f(m)11}$	J/m-sec-c	Btu/hr/ft^2/^{o}F/in.	1.09×10^9	580.	2.35×10^6	[a]1.25
	$\kappa_{f(m)22}$	J/m-sec-c	Btu/hr/ft^2/^{o}F/in.	1.09×10^8	58.	2.35×10^6	[a]1.25
	$\kappa_{f(m)33}$	J/m-sec-c	Btu/hr/ft^2/^{o}F/in.	1.09×10^8	58.	2.35×10^6	[a]1.25
Weight density	$\rho_{f(m)}$	g/cm^3	lb/in.^{3}	1.8	.065	1.2	.044

[a]Estimated.

Notation: f(m) denotes fiber or matrix property.

TABLE 4. - CONSTITUENT PROPERTIES FOR MICROMECHANICS STRENGTH PREDICTIONS

Property	Symbol	Units		Value	
		SI	Customary	SI	Customary
Fiber tensile strength	S_{fT}	10^3N/cm^2	ksi	242	350
Matrix compressive strength	S_{mC}	10^3N/cm^2	ksi	11.3	16.5
Matrix tensile strain	ϵ_{mpT}	cm/cm	in./in.	.018	.018
Matrix compressive strain	ϵ_{mpC}	cm/cm	in./in.	.035	.035
Matrix shear strain	ϵ_{mpS}	cm/cm	in./in.	.050	.050
Matrix torsional strain	ϵ_{mpTOR}	cm/cm	in./in.	.050	.050

TABLE 5. - MICROMECHANICS STRENGTH
CORRELATION COEFFICIENTS

Coefficient	Symbol	Value
Longitudinal tensile strength	β_{fT}	.94
	β_{mT}	1.00
Longitudinal compressive strength		
Matrix compression limited	β_{fC}	.17
	β_{mC}	1.00
Intralaminar shear limited	a_1	13.30
	a_2	31900
Transverse tensile strength	β_{22T}	1.06
Transverse compressive strength	β_{22C}	1.60
Intralaminar shear strength	β_{12S}	1.00
Delamination	β_{DEL}	16.5

TABLE 6. - HT-S/PMR-PI MEASURED AND PREDICTED UNIDIRECTIONAL COMPOSITE MECHANICAL PROPERTIES
FOR A .55 FIBER VOLUME RATIO COMPOSITE.

Property	Symbol	Unit		Measured		Predicted	
		SI	Customary	SI	Customary	SI	Customary
Longitudinal modulus	E_{l11}	$10^6 N/cm^2$	10^6 psi	15.0	21.7	14.5	21.1
Transverse modulus	E_{l22}	$10^6 N/cm^2$	10^6 psi	.83	1.2	.83	1.2
Shear modulus	G_{l12}	$10^6 N/cm^2$	10^6 psi	----	----	.50	.72
Poisson's ratio	ν_{l12}	Ratio	Ratio	----	----	.24	.24
Longitudinal thermal coef. of exp.	α_{l11}	10^{-6}cm/cm/C	10^{-6}in./in./^oF	~0	~0	.49	.27
Transverse thermal coef. of exp.	α_{l22}	10^{-6}cm/cm/C	10^{-6}in./in./^oF	25.6	14.2	26.1	14.5
Longitudinal thermal heat conductivity	K_{l11}	J/m-sec-c	Btu/hr/ft^2/^oF/in.	----	----	6.02×10^8	320
Transverse thermal heat conductivity	K_{l22}	J/m-sec-c	Btu/hr/ft^2/^oF/in.	----	----	8.27×10^6	4.4
Through-the-thickness thermal heat conductivity	K_{l33}	J/m-sec-c	Btu/hr/ft^2/^oF/in.	----	----	8.27×10^6	4.4
Longitudinal tensile strength	S_{l11T}	$10^3 N/cm^2$	ksi	125	182	126	183
Longitudinal compressive strength	S_{l11C}	$10^3 N/cm^2$	ksi	94	136	95	138
Transverse tensile strength	S_{l22T}	$10^3 N/cm^2$	ksi	6.6	9.6	6.2	9.0
Transverse compressive strength	S_{l22C}	$10^3 N/cm^2$	ksi	23.4	[a]34.0	18.0	[c]26.1
Intralaminar shear strength	S_{l12S}	$10^3 N/cm^2$	ksi	11.0	[b]16.0	5.5	[d]8.0
Coefficient for combines stress	K_{l12}	Ratio	Ratio	----	----	1.09	1.09

[a]Maximum value with considerable nonliniarity.
[b]Short-beam-shear stress.
[c]About 80% of maximum value was used.
[d]One-half of short-beam-shear stress was used.

TABLE 7. - LAMINATE ELASTIC CONSTANTS AND THERMAL COEFFICIENTS OF EXPANSION

[HT-S/PMR-PI; fiber volume ratio = .55; weight density = 1.6 g/cm^3 (.056 lb/in.^{3})]

Laminate	Moduli: 10^6N/cm^2/(10^6 psi)			Poisson's ratio	Thermal coefficients of expansion 10^{-6}cm/cm/C(in./in./^{o}F)	
	E_{cxx}	E_{cyy}	G_{cxy}	ν_{cxy}	α_{cxx}	α_{cyy}
6[0]	14.5	0.83	0.50	0.24	0.49	26.1
	21.1	1.20	.72	.24	.27	14.5
4[+ 10, - 10, - 10, + 10]	13.4	.83	.90	.68	-.11	25.0
	19.4	1.20	1.30	.68	-.06	13.9
8[0, + 10, 0, - 10, - 10, 0, + 10, 0]	14.0	.83	.69	.46	.02	25.6
	20.3	1.20	1.00	.46	.01	14.2
13[+ 40, - 40, 9(0), - 40, + 40]	11.0	1.52	1.45	.73	-.13	13.0
	16.0	2.20	2.1	.73	-.07	7.2
4[+ 40, - 40, - 40, + 40]	2.3	1.4	3.65	1.00	-.70	6.03
	3.4	2.0	5.30	1.00	-.39	3.35

TABLE 8. - LAMINATE 13[$\pm$ 40, 9(0) $\mp$ 40] AXIAL AND BENDING STIFFNESS.

[HT-S/PMR-PI; fiber volume ratio = .55; weight density = 1.6 g/cm^3 (.056 lb/in.^{3})]

Stiffness (see schematic)	Symbol	Units		Value	
		SI	Customary	SI	Customary
Bending along-x	D_{c11}	CM-N	IN.-LB	14377	1272
Bending along-y	D_{c22}	CM-N	IN.-LB	4160	368
Coupled bending x with y	D_{c12}	CM-N	IN.-LB	3832	339
Coupled x-bending with twisting	D_{c13}	CM-N	IN.-LB	780	69
Coupled y-bending with twisting	D_{c23}	CM-N	IN.-LB	565	50
Twisting	D_{c33}	CM-N	IN.-LB	4318	382

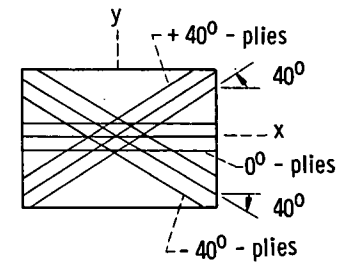

Ply orientation schematic

TABLE 9. - PLY STRESSES IN LAMINATE 6(0).

[HT-S/PMR-PI .55 fiber volume ratio. Ply stress in $10^3 N/cm^2$ first line, ksi second line.]

Laminate load/ply	Thermal load due to cure ΔT = -294.5C (-530°F)				Mechanical load				Combined loads			
	σ_{l11}	σ_{l22}	σ_{l12}	MOS	σ_{l11}	σ_{l22}	σ_{l12}	MOS	σ_{l11}	σ_{l22}	σ_{l12}	MOS
N (lb)												
42 200 (9500)												
All plies	0	0	0	1.00	128	0	0	-.04	128	0	0	-.04
	0	0	0	1.00	186	0	0	-.04	186	0	0	-.04
N-cm (lb-in.)												
1030 (91)												
Bottom ply	0	0	0	1.0	121	0	0	.09	121	0	0	.09
	0	0	0	1.0	175	0	0	.09	175	0	0	.09
Top ply	0	0	0	1.0	-121	0	0	-1.20	-121	0	0	-1.20
	0	0	0	1.0	-175	0	0	-1.20	-175	0	0	-1.20

TABLE 10. - PLY STRESSES IN LAMINATE 4($\pm$ 10, $\mp$ 10).

[HT-S/PMR-PI .55 fiber volume ratio. Ply stress in $10^3 N/cm^2$ first line, ksi second line.]

Laminate load/ply	Thermal load due to cure ΔT = -294.5C (-530°F)				Mechanical load				Combined loads			
	σ_{l11}	σ_{l22}	σ_{l12}	MOS	σ_{l11}	σ_{l22}	σ_{l12}	MOS	σ_{l11}	σ_{l22}	σ_{l12}	MOS
N (lb)												
24 910 (5600)												
+ 10	-.5	.5	-1.2	.94	104	-2.5	-2.1	.04	103	-2.0	-3.4	-1.57
	-.7	.7	-1.8	.94	151	-3.6	-3.1	.04	150	-2.9	-4.9	-1.57
- 10	-.5	.5	1.2	.94	104	-2.5	2.1	.04	103	-2.0	3.4	-1.57
	-.7	.7	1.8	.94	151	-3.6	3.1	.04	150	-2.9	4.9	-1.57
N-cm (lb-in.)												
622 (55)												
Bottom + 10	-.5	-.5	-1.2	.94	104	.5	-12.6	-4.98	105	.9	-13.8	-6.07
	-.7	-.7	-1.8	.94	153	.7	-18.3	-4.98	153	1.3	-20.1	-6.07
Top + 10	-.5	-.5	-1.2	.94	-104	-.5	12.6	-5.98	-106	~0	11.4	-5.01
	-.7	-.7	-1.8	.94	-153	-.7	18.3	-5.98	-154	~0	16.5	-5.01

TABLE 11. - PLY STRESSES IN LAMINATE 8[0, + 10, 0, - 10, - 10, 0, + 10, 0].

[HT-S/PMR-PI .55 fiber volume ratio. Ply stress in $10^3 N/cm^2$ first line, ksi second line.]

Laminate load/ply	Thermal load due to cure ΔT = -294.5C (-530°F)				Mechanical load				Combined loads			
	σ_{l11}	σ_{l22}	σ_{l12}	MOS	σ_{l11}	σ_{l22}	σ_{l12}	MOS	σ_{l11}	σ_{l22}	σ_{l12}	MOS
N (lb)												
63 500 (14 270)												
0	1.4	.1	~0	1.00	135	-1.7	~0	-.31	136	-1.5	~0	-.26
	2.0	.2	~0	1.00	196	-2.5	~0	-.25	198	-2.2	~0	-.26
+ 10	-1.9	.3	-1.2	.94	130	-1.4	-2.3	-.31	128	-1.1	-3.6	-.51
	-2.7	.5	-1.8	.94	188	-2.1	-3.4	-.31	185	-1.6	-5.2	-.51
- 10	-1.9	.3	1.2	.94	130	-1.4	2.3	-.31	128	-1.1	3.6	-.51
	-2.7	.5	1.8	.94	188	-2.1	3.4	-.31	185	-1.6	5.2	-.51
N-cm (lb-in.)												
2113 (187)												
Bottom 0	1.4	.1	~0	1.0	128	-.7	-4.3	-.68	129	-.5	-4.3	-.69
	2.0	.2	~0	1.0	185	-1.0	-6.3	-.68	187	-.7	-6.3	-.69
+ 10	-1.9	.3	-1.2	.94	72	.3	-4.3	.64	70	.6	-5.6	-.33
	-2.7	.5	-1.8	.94	104	.5	-6.3	.64	102	.9	-8.1	-.33
Top 0	1.4	.1	~0	1.0	-128	.7	4.3	-2.23	-126	.9	4.3	-2.22
	2.0	.2	~0	1.0	-185	1.0	6.3	-2.23	-183	1.3	6.3	-2.22
+ 10	-1.9	.3	-1.2	.94	-72	.3	4.3	-.40	-74	~0	3.0	-.14
	-2.7	.5	-1.8	.94	-104	.5	6.3	-.40	-107	~0	4.4	-.14

TABLE 12a. - PLY STRESSES IN LAMINATE 13[+ 40, - 40, 9(0), - 40, + 40].

[HT-S/PMR-PI .55 fiber volume ratio. Ply stress in $10^3 N/cm^2$ first line, ksi second line.]

Laminate load/ply	Thermal load due to cure ΔT = -294.5C (-530°F)				Mechanical load				Combined loads			
	σ_{l11}	σ_{l22}	σ_{l12}	MOS	σ_{l11}	σ_{l22}	σ_{l12}	MOS	σ_{l11}	σ_{l22}	σ_{l12}	MOS
N (lb)												
57 840 (13 000)												
+ 40	-19.4	4.3	-1.9	.21	31.7	.3	-6.4	-.44	12.3	4.6	-8.3	-1.80
	-28.1	6.2	-2.7	.21	46.0	.5	-9.3	-.44	17.9	6.7	-12.1	-1.80
- 40	-19.4	4.3	1.9	.21	31.7	.3	6.4	-.44	12.3	4.6	8.3	-1.80
	-28.1	6.2	2.7	.21	46.0	.5	9.3	-.44	17.9	6.7	12.1	-1.80
0	3.4	3.2	~0	.74	110.2	-3.1	~0	.07	113.7	.2	~0	.20
	5.0	4.7	~0	.74	160.0	-4.5	~0	.07	165	.3	~0	.20

TABLE 12b. - PLY STRESSES IN LAMINATE 13[+ 40, - 40, 9(0), - 40, + 40]

[HT-S/PMR-PI .55 fiber volume ratio. Ply stress in $10^3 N/cm^2$ first line, ksi second line.]

Laminate load/ply	Thermal load due to cure ΔT = -294.5C (-530°F)				Mechanical load				Combined loads			
	$\sigma_{\ell 11}$	$\sigma_{\ell 22}$	$\sigma_{\ell 12}$	MOS	$\sigma_{\ell 11}$	$\sigma_{\ell 22}$	$\sigma_{\ell 12}$	MOS	$\sigma_{\ell 11}$	$\sigma_{\ell 22}$	$\sigma_{\ell 12}$	MOS
N-cm (lb-in.)												
1854 (164)												
Bottom + 40	-19.4	4.3	-1.9	.21	21.9	-.3	7.8	-1.11	2.6	3.9	-9.8	-2.57
	-28.1	6.2	-2.7	.21	31.8	-.5	11.4	-1.11	3.7	5.7	-14.2	-2.57
- 40	-19.4	4.3	1.9	.21	25.4	-.6	6.5	-.46	5.2	3.7	8.3	-1.67
	-28.1	6.2	2.7	.21	35.5	-.8	9.4	-.46	7.5	5.4	12.1	-1.67
0	3.4	3.2	~0	.74	80.6	-3.1	-.2	.45	84.1	.1	-.1	.56
	5.0	4.7	~0	.74	117	-4.5	-.3	.45	122	.2	-.2	.56
Top + 40	-19.4	4.3	-1.9	.21	-21.9	.3	7.8	-1.17	-41.2	4.5	6.0	-1.36
	-28.1	6.2	-2.7	.21	-31.8	.5	11.4	-1.17	-59.8	6.6	8.7	-1.36
- 40	-19.4	4.3	1.9	.21	25.4	.6	-6.5	-.53	-43.8	4.8	-4.6	-.99
	-28.1	6.2	2.7	.21	35.5	.8	-9.4	-.53	-63.6	7.0	-6.7	-.99
0	3.4	3.2	~0	.74	-80.6	3.1	.2	-.68	77.2	6.3	.2	-1.86
	5.0	4.7	~0	.74	-117	4.5	.3	-.68	-112	9.2	.3	-1.86

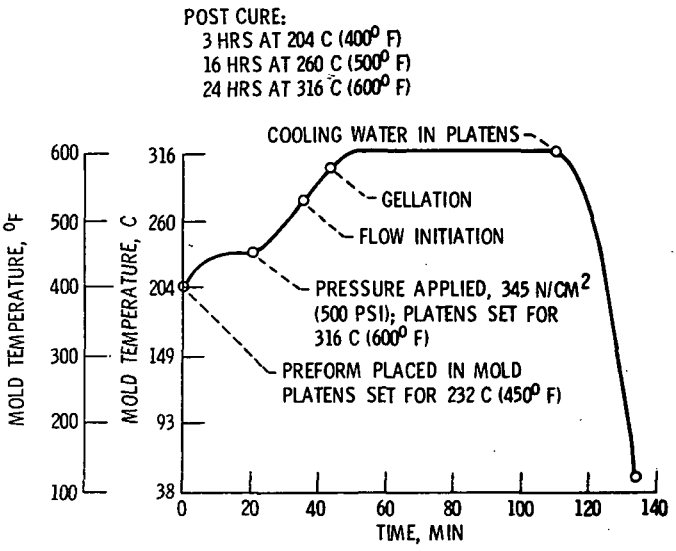

Figure 1. - Molding cycle for PMR-PI laminate.

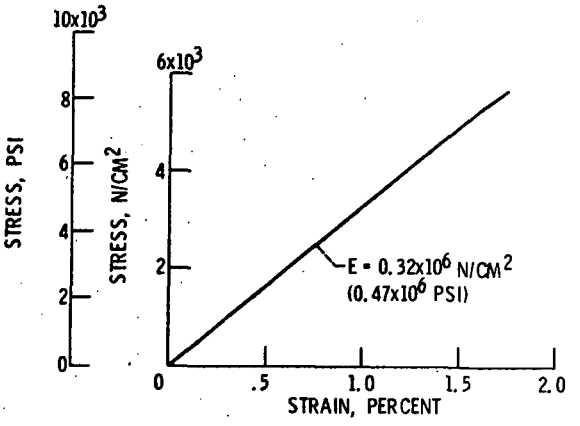

Figure 2. - Stress-strain diagram of PMP-PI neat resin at room temperature.

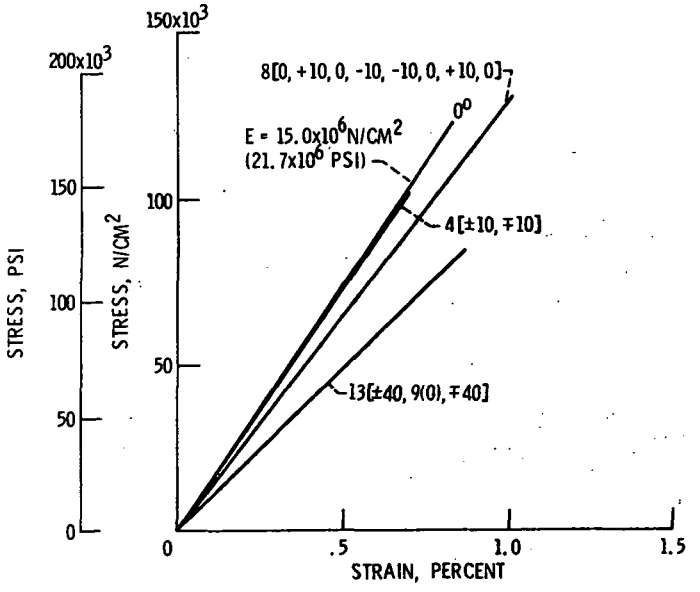

Figure 3. - Stress-strain diagram of various HT-S/PMR-PI angleplied laminates at room temperature.

E-7700

NASA-Lewis